Journal of Nuclear Materials 395 (2009) 79–88

Contents lists available at ScienceDirect

Journal of Nuclear Materials

journal homepage: www.elsevier.com/locate/jnucmat

Thermodynamic assessment of the Pd–H–D–T system

J.-M. Joubert [a,*], S. Thiébaut [b]

[a] Chimie Métallurgique des Terres Rares, Institut de Chimie et des Matériaux Paris-Est, CNRS, Université de Paris XII, UMR 7182, 2-8 rue Henri Dunant, F-94320 Thiais, France
[b] CEA/DAM/Valduc, F-21120 Is sur Tille, France

ARTICLE INFO

Article history:
Received 16 June 2009
Accepted 29 September 2009

PACS:
02.60.Ed
05.70.−a
28.52.Fa
28.60.+s
64.75.Cd
82.60.Lf

ABSTRACT

The three binary systems H–Pd, D–Pd and Pd–T have been modelled in the frame of the Calphad approach. A complete literature search has been undertaken and the most significant experimental data have been selected for a thermodynamic assessment of these systems. To complement the available data, pressure–composition curves have been measured for the three systems in the present work. The three systems are characterized by a strong isotope effect which is well taken into account in the modelling. They have been combined to perform calculations in the quaternary H–D–Pd–T system. It is shown that a reasonable extrapolation can be made without the use of ternary parameters if it is calculated with the so-called Toop model.

1. Introduction

Research on metal–hydrogen systems is motivated by the many fundamental properties and possible applications of these systems among which hydrogen storage, metal–hydride batteries, hydrogen purification and gettering. The thermodynamic modelling of such systems by the Calphad method has recently become a very active field [1–15]. Palladium–hydrogen system can be considered as a model for all the metal–hydrogen systems. It has been the most studied system in particular because it is easy to study experimentally. It combines high kinetics, easy activation and low oxidation. The phase diagram is relatively simple, at least at moderate temperatures. It is characterized by the classical miscibility gap between hydrogen poor and rich compositions. The equilibrium between these two compositions occurs at a constant, so-called, plateau pressure. In spite of its apparent simplicity, Pd–H system possesses incredibly rich chemistry (Pd is the only element absorbing and desorbing hydrogen at room temperature) and physics (superconductivity, low temperature ordering). Additionally, Pd is the only element that does no pulverize after hydrogen insertion yielding interesting applications in hydrogen purification since membranes can be manufactured.

Generally, changing an element by its isotope does not influence the thermodynamic properties. However, hydrogen is the only element for which the mass ratio between isotopes can reach 2 (for deuterium) or even 3 (for tritium). This has severe consequences in particular in the case of palladium for which the plateau pressure is multiplied by a factor of almost ten between hydrogen and tritium systems. This makes palladium very attractive for isotope separation.

Tritium is considered as a fuel for future thermonuclear power plants. Tritium storage in palladium offers a safe and compact solution to the problem of handling this gas with specific radioactivity. In addition, ^{3}He associated with tritium decay is trapped in Pd offering the possibility to recover very pure gas. Generally, the presence of ^{3}He, insoluble in metals, generates structural defects and induces changes in their storage properties (the phenomena associated with the presence of ^{3}He in metals are called "ageing"). But in the case of Pd, ageing induces very few changes, in particular of the storage properties, compared to what is observed in other hydride forming metals or compounds such as Ti [16] or $LaNi_5$ [17] even for long term storage.

The modelling of Pd–H–D–T system is very important in particular because experiments with tritium are very difficult to undertake. Modelling will allow the calculation of the isotope separation factor at any temperature, pressure and overall H, D, T content offering the possibility to find optimized conditions for separation. It will allow as well the prediction of the nature of the species formed in the gas phase at the equilibrium among H_2, D_2, T_2, HD, HT, DT. It has been conducted in this work in the frame of the Calphad approach. This method consists in fitting the parameters describing the Gibbs energy of the different phases of the system to the experimental data by a least-square procedure. When the parameters are obtained, the calculation of various thermodynamic quantities can be performed (phase diagram, enthalpies)

* Corresponding author. Tel.: +33 1 49 78 12 11; fax: +33 1 49 78 12 03.
E-mail address: jean-marc.joubert@icmpe.cnrs.fr (J.-M. Joubert).

0022-3115/$ - see front matter © 2009 Elsevier B.V. All rights reserved.
doi:10.1016/j.jnucmat.2009.09.021

and the Gibbs energies relative to different systems can be combined in order to obtain reliable extrapolations in higher order systems.

2. Literature review and selection of data

We review the data available for the different systems studied. The list of the experimental data used in the present assessments is given in Table 1.

2.1. Pd–H system

This system has been extensively studied. It is not the purpose of this work to make an exhaustive review of the existing data. Such reviews are already available in Refs. [18,19], but the most complete description of the system from the phase diagram and thermodynamic point of view is the one by Manchester et al. [20]. We will describe mainly the data selected for the optimization.

2.1.1. Phase diagram

The phase diagram of the Pd–H system is a simple miscibility gap [20]. Hydrogen poor and rich compositions on the two sides of the miscibility gap are generally named α and β phases, though this appellation is very confusing since both names refer to the same phase. The position of the critical point has been evaluated by different techniques mostly based on extrapolations. The recommended values are $T_c = 566$ K, $x_C = 0.22$, $P_C = 20.15 \times 10^5$ Pa [21]. Since these are derived data, they will not be used in the assessment of the system.

The limits of the miscibility gap have generally been determined as the inflexion points on the pressure–composition curves at different temperatures [22,23]. The limit between the solubility branch and the pressure plateau corresponding to the phase transition characteristic of the miscibility gap is often difficult to locate precisely. More abrupt changes are observed for the magnetic susceptibility as a function of composition. This allows to define more accurately the composition limits [24,25]. All the data from these four references are compatible and have been used in the assessment.

Table 1
Experimental data used in the present assessment.

Type of data	System	Temperature domain (K)	Reference
Miscibility gap	Pd–H, Pd–D	$195 < T < 348$	[22]
	Pd–H	$287 < T < 363$	[23]
	Pd–H	$293 < T < 561$	[24]
	Pd–D, Pd–T	$323 < T < 393$	[41]
	Pd–D	$343 < T < 553$	[42]
	Pd–H	$T = 273$	[25]
Pressure–composition–temperature data	Pd–H, Pd–D	$195 < T < 348$	[22]
	Pd–H	$273 < T < 363$	[23]
	Pd–H, Pd–D	$167 < T < 333$	[30]
	Pd–H	$293 < T < 571$	[24]
	Pd–H	$393 < T < 473$	[31]
	Pd–D	$T = 555$	[43]
	Pd–T	$298 < T < 343$	[45]
	Pd–D	$700 < T < 909$	[36]
	Pd–D, Pd–T	$303 < T < 433$	[44]
	Pd–H, Pd–D	$433 < T < 593$	[32]
	Pd–T	$333 < T < 673$	[46]
	Pd–D	$303 < T < 613$	[42]
	Pd–T	$423 < T < 673$	[47]
	Pd–T	$273 < T < 393$	[48]
	Pd–T	$298 < T < 313$	[49]
	Pd–H	$T = 303$	[33]
	Pd–T	$413 < T < 473$	[50]
	Pd–H, Pd–D, Pd–T	$239 < T < 471$	This work
Calorimetric measurements	Pd–H	$T = 323$	[37]
	Pd–H	$T = 689$	[35]
	Pd–H	$518 < T < 625$	[38]
	Pd–H, Pd–D	$555 < T < 909$	[36]
	Pd–H, Pd–D	$518 < T < 593$	[39]
	Pd–H, Pd–D	$T = 298$	[40]
	Pd–H	$T = 303$	[33]

2.1.2. Crystal structure

Pd is *fcc* and hydrogen in Pd(H) solid solutions is located in interstitial sites. Neutron diffraction studies have shown that hydrogen atoms are located in octahedral sites both in hydrogen rich [26] and hydrogen poor [27] solid solutions. In these two studies both hydrogen and deuterium solid solution were studied and, as usual for metal hydrides, the crystal structure properties are identical. As deuterides are much easier to study due to the incoherent scattering of hydrogen, most structural studies are devoted to deuterium solid solutions. No long range ordering has been evidenced at any composition around room temperature or above. For a complete review of the structural studies made on palladium hydride and deuteride, one may refer to Ref. [28]. The complete occupancy of the octahedral sites limits the composition of the stoichiometric hydride to be PdH. As this composition may be approached at high pressures, several studies were undertaken to investigate the possibility of additional insertion in the tetrahedral sites. The tetrahedral occupancy has been evidenced in only one case in the most recent and careful study [28]. However, it is claimed that this occupancy is due to a special sample preparation (samples loaded in the supercritical region) and the tetrahedral occupancy remains quite small as compared the octahedral occupancy (around 10%).

Low temperature superstructures have been evidenced when samples are cooled below 85 K due to hydrogen ordering. For a review, the reader is referred to Ref. [20]. They will not be considered in the present work.

2.1.3. Pressure–composition curves

The pressure–composition curves measured at temperatures below the critical point are characterized by the presence of a pressure plateau corresponding to the transition between the two composition sets defined by the miscibility gap. A lot of these curves have been measured in isothermal conditions, a few in isochoral conditions, most of them with the Sieverts method [29]. We selected the most accurate data. In Refs. [22–24,30–33], the whole pressure–composition curves, solubility curves in the hydrogen poor or rich regions, or only plateau pressures have been measured. Additionally, several isothermal pressure–composition curves have been measured in the present work in volumetric devices with the Sieverts method.

The pressure–composition curves are characterized by the presence of a strong hysteresis between absorption and desorption. When available both data have been taken into account. We have limited our study to moderate temperatures. Solubilities in solid and liquid palladium at very high temperatures (1573–2503 K) [34] have not been considered in this work.

2.1.4. Thermodynamic measurements

Thermodynamic data derived from pressure–composition–temperature measurements are presented in many papers. They have not been used, since it is preferable to optimize the original pressure–composition data points. The derived data can however be used for comparison purposes with the calculated thermodynamic data (see *e.g.* the comparison of enthalpy at infinite dilution).

Partial enthalpies as a function of composition have been measured by calorimetry in low H concentration [33,35,36] and both low and high H concentration [37–39] solubility branches. Flanagan et al. have measured the enthalpy in the complete composition range *i.e.* also across the transformation plateau [40]. It is evidenced that the enthalpy is the same during absorption and desorption. Unlike pressure–composition curves it does not show hysteresis. This result shows not only that calorimetric data are more suitable than pressure–composition data to represent the thermodynamics of the system but also that the real equilibrium plateau pressure is neither absorption nor desorption pressure, as several authors claim, but lies in between. As a consequence, in the present assessment, the calorimetric data will be preferred over the pressure–composition data when possible.

2.1.5. Modelling

An assessment of the Pd–H system by Huang et al. has recently been published [9]. Comparison will be made between the two assessments in the following.

2.2. Pd–D system

Pd–H and Pd–D systems are pretty similar. The most remarkable change is the magnitude of the plateau pressure. The issues addressed for Pd–H system which remains valid for the Pd–D system will not be repeated (crystal structure, presence of the hysteresis, absence of hysteresis in the calorimetric data). Neither a complete review nor a thermodynamic assessment is available for this system.

2.2.1. Phase diagram

Only slight differences can be noted between the Pd–H and Pd–D phase diagrams. Different values of the critical temperature have been stated but the difference does not exceed 10 K [20]. Like for Pd–H system, the determination of the miscibility gap has been made from the observation of the pressure–composition curves [22,41]. However, the most significant contribution to this system is the one of Blaurock [42]. This author used the same susceptibility technique as Frieske and Wicke [24] for the determination of the miscibility gap. He evidenced differences between absorption and desorption.

2.2.2. Pressure–composition curves

We selected the following data: [22,30,32,36,42–44]. As for hydrogen, several pressure–composition curves have been measured in the present work. If the phase diagrams of Pd–H and Pd–D are very similar, on the contrary, the plateau pressures of the pressure–composition curves are affected by a huge isotope effect (they are approximately 5 times higher for deuterium than for hydrogen).

2.2.3. Thermodynamic measurements

The available thermodynamic properties are more limited than for hydrogen. Only two paper reports the partial enthalpies in dilute solid solutions at high temperature [36,39], while Flanagan et al. have measured the enthalpy in the complete composition range as for hydrogen [40].

2.3. Pd–T system

Due to the specific radioactivity of tritium, experimental measurements on the Pd–T system are very difficult to perform. This is the reason why only few papers are devoted to the study of this system. In this respect, we should emphasize the extensive work made by Lässer. In addition to the difficulty of handling radioactive materials, other experimental problems are raised by the isotopic purity of the gas. Tritium is always associated with the presence of hydrogen and deuterium which may affect the measured quantities (in particular the pressure in the solubility branches). Some papers consider corrections due to this isotopic purity, other do not. Another difficulty is associated with the chemical purity of tritium due to its radioactive decay into ^{3}He. The presence of ^{3}He may also affect the measurements of the equilibrium pressures.

Few data exist on the miscibility gap [41]. Pressure–compositions curves have been measured in the low T concentration region [45,46], or in the complete concentration range [44,47–50]. As for the two previous systems, we have measured pressure–composition curves. The precise experimental procedure is given in Ref. [49]. The most important point to notice is that the gas used contains less than 1 at.% H, less than 2 at.% of both H and D and less than 1 at.% ^{3}He, so corrections are not necessary. Moreover, the gas composition is measured by mass spectrometry for each equilibrium point, so pressure in the pressure–composition curves corresponds to the partial pressure of H, D and T, not to the total pressure (to which high partial ^{3}He pressure can contribute).

The plateau pressures are even higher in the Pd–T system (approximately 10 times higher than for hydrogen). No previous assessment of this system has been published.

2.4. Pd–H–D, Pd–H–T and Pd–D–T

Information on the ternary systems are of two kinds: measurement of the isotope separation factor [22,51–54] and measurement of mixed pressure–composition curves [55,56]. The isotope separation factor is defined as the ratio between hydrogen to deuterium content in the solid and the gas phase:

$$\alpha = \frac{x_{\mathrm{H}}^{fcc}}{x_{\mathrm{D}}^{fcc}} \frac{x_{\mathrm{D}}^{\mathrm{gas}}}{x_{\mathrm{H}}^{\mathrm{gas}}} \tag{1}$$

In general, in the above papers, the experimental conditions have not been detailed sufficiently to perform exact comparison between calculated and experimental values. For the measurement of the separation factor, the ratio between the number of moles in the gas and in the solid phase is important and has been sometimes disregarded. For the measurement of pressure–composition curves, the knowledge of the path followed in the ternary systems is of primary importance. If the composition of the gas is changing during the measurement, the resulting plateau in the pressure–composition curves may show a slope which is impossible to reproduce by calculation without knowing the volumes of the systems and the ratio between the number of moles in the gas and solid phases at each step.

This is the reason why, in the present work, the value of the plateau pressure for hydrogen–deuterium mixing has been measured. With our experimental set-up, it was not possible to measure the isotope ratio in the gas phase. Therefore, our measurement has been performed in absorption only. We have used a large weight of palladium so that the number of moles in the gas phase after absorption is negligible. Hence, the isotope ratio in the solid corresponds to the isotope mixing introduced before absorption.

3. Thermodynamic modelling

3.1. The Calphad method

For a complete description of the Calphad methodology, the reader is referred to textbooks such as Ref. [57]. This method consists in assessing the Gibbs energy of each phase of the system. The Gibbs energies are described by equations with parameters that are adjusted by a least-square method in order to reproduce as well as possible the available thermodynamic or phase diagram data. After assessment of simple systems, these can be combined to predict phase equilibria in higher order systems.

3.2. Gas phase

The gas phase has been considered as ideal. We limit the modelling to moderate temperatures and pressures. The correction for non-ideality of the Gibbs energy of hydrogen gas is significant only far above 100 or 1000 bar and far below 300 K [58]. Given the very low vapour pressure of Pd for the considered temperature range, the only species considered are the diatomic molecular species H_2, D_2, T_2, HD, HT and DT. The values of the Gibbs energy of these species in their stable-element reference (SER) state at 298.15 K and $P_0 = 10^5$ Pa have been taken from the PURE [59] and SSUB4 [60] databases.

For pure hydrogen, the Gibbs energy can be written as:

$$G^{\text{gas}} = G^{\text{SER}}_{H_2} + RT\ln(P/P_0) \tag{2}$$

3.3. Solid phase

Though evidenced by Pitt, but in a special occasion, the minoritary tetrahedral occupancy by H and its isotopes will be neglected. We will therefore consider the unique solid phase of this system as an interstitial solid solution of H, D and T in *fcc* palladium. This choice is justified not only by the fact that the limiting composition PdH is never overcome but also by the many structural studies we have detailed above. We have used the sublattice model expressed in the compound energy formalism [61]. The model is therefore: Pd:H, D, T, vac where the semi-column separates the two sublattices, the commas separate the elements sharing a same sublattice and vac stands for vacancy.

For the binary Pd–H system (similar equations are used for Pd–D and Pd–T systems), the Gibbs energy of the solid phase is described as a function of the site fractions of hydrogen and vacancies in the octahedral sites (y_H and y_{vac}) and temperature, and modelled as the sum of the reference (ref), ideal (id) and excess (ex) parts:

$$G^{fcc} = {}^{\text{ref}}G^{fcc} + {}^{\text{id}}G^{fcc} + {}^{\text{ex}}G^{fcc} \tag{3}$$

where

$${}^{\text{ref}}G^{fcc} = y_{vac}G^{fcc}_{Pd} + y_H G^{fcc}_{Pd:H} \tag{4}$$

G^{fcc}_{Pd} is taken from the PURE database [59]. $G^{fcc}_{Pd:H}$ is the Gibbs energy of formation of the hypothetical compound PdH from *fcc* Pd and H (*a*, *b*, *c* and *d* are the parameters to be optimized):

$$G^{fcc}_{Pd:H} = G^{fcc}_{Pd} + \frac{1}{2}G^{\text{SER}}_{H_2} + a + bT + cT\ln(T) + dT^2 \tag{5}$$

The ideal Gibbs energy is associated with the mixing entropy of the species H and vac in the second sublattice:

$${}^{\text{id}}G^{fcc} = RT(y_H \ln y_H + y_{vac}\ln y_{vac}) \tag{6}$$

The non-ideal part of the Gibbs energy is described with the Redlich–Kister model [62] following:

$${}^{\text{ex}}G^{fcc} = y_H y_{vac}\sum_{v=0}^{n} {}^{v}L^{fcc}_{H,vac}(y_H - y_{vac})^v \tag{7}$$

$${}^{v}L^{fcc}_{H,vac} = {}^{v}a^{fcc} + {}^{v}b^{fcc}T \tag{8}$$

The miscibility gap arises from peculiar values of these interaction (repulsive) parameters. Finally, the occupancy parameter and the composition of hydrogen in the solid phase are related by:

$$x^{fcc}_H = \frac{y_H}{1 + y_H} \tag{9}$$

3.4. Optimization

The three binary systems have been modelled independently using the Parrot module [63] of Thermocalc [64]. In the final stage of the optimization, all the experimental data described above and in Table 1 have been assessed with weights corresponding to the estimated uncertainties and the relative importance of the measurement until a set of parameters is able to describe all the data sufficiently well. Finally, the optimized parameters were rounded off to the last significant digit and are presented in Table 2.

As shown by Flanagan et al. [40], in the plateau region neither the absorption nor the desorption pressure–composition curves represent the true equilibrium. Contrary to these, the calorimetric data do not show any hysteresis. There are therefore more suited to describe the real equilibrium and higher weight has been put on these data for the optimization of the two systems in which they were available (Pd–H and Pd–D).

The non-symmetrical miscibility gaps are described by using interaction parameter up to ${}^{2}L$, each with temperature dependence. This has been found to be necessary especially to model the curvature of the pressure–composition curves in the hydrogen-rich region. The variation of the partial enthalpy as a function of temperature had to be described by adding terms in $T\ln(T)$ and T^2 in the description of the Gibbs energy of the end-member Pd:H. In the Pd–T system, because of few available experimental data, all the interaction parameters and the terms in $T\ln(T)$ and T^2 have been kept equal to the values obtained for the Pd–D system.

4. Results and discussion

4.1. Pd–H system

The calculated phase diagram of the Pd–H system is drawn in Fig. 1 with a comparison of the experimental data describing the

Table 2
List of the optimized parameters (in J mol^{-1}).

$G^{fcc}_{Pd:H} = G^{fcc}_{Pd} + \frac{1}{2}G^{SER}_{H_2} - 14550 + 39.7T + 2.6T\ln(T) - 0.0122T^2$
$G^{fcc}_{Pd:D} = G^{fcc}_{Pd} + \frac{1}{2}G^{SER}_{D_2} - 12200 + 37.5T + 2.68T\ln(T) - 0.0122T^2$
$G^{fcc}_{Pd:T} = G^{fcc}_{Pd} + \frac{1}{2}G^{SER}_{T_2} - 11500 + 37.94T + 2.68T\ln(T) - 0.0122T^2$
${}^{0}L^{fcc}_{H,vac} = -7390 + 10.1T$
${}^{1}L^{fcc}_{H,vac} = -21090 + 19.6T$
${}^{2}L^{fcc}_{H,vac} = -9400 + 13.7T$
${}^{0}L^{fcc}_{D,vac} = -9150 + 15.3T$
${}^{1}L^{fcc}_{D,vac} = -21280 + 21.4T$
${}^{2}L^{fcc}_{D,vac} = -8550 + 12.5T$
${}^{0}L^{fcc}_{T,vac} = -9150 + 15.3T$
${}^{1}L^{fcc}_{T,vac} = -21280 + 21.4T$
${}^{2}L^{fcc}_{T,vac} = -8550 + 12.5T$

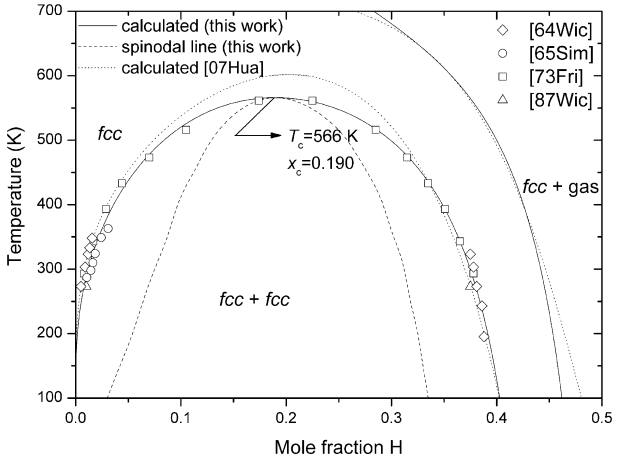

Fig. 1. Pd–H phase diagram at 1×10^7 Pa. The calculated spinodal line and the phase diagram calculated by [07Hua, [9]] are shown. Experimental data from [64Wic, [22]], [64Sim, [23]], [73Fri, [24]] and [87Wic, [25]] are represented.

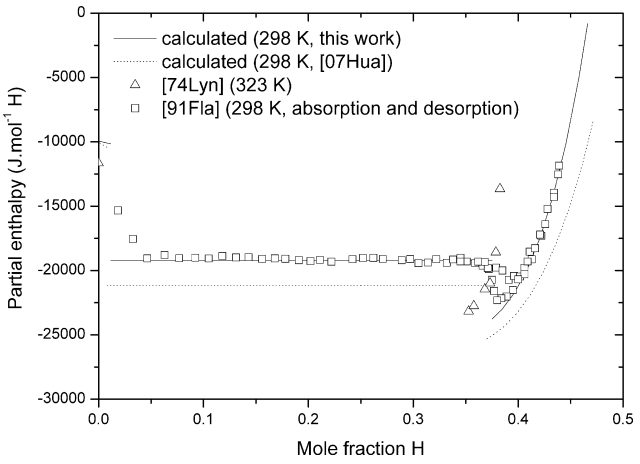

Fig. 2. Partial enthalpy at low temperature as a function of composition in the Pd–H system. Experimental data from [74Lyn, [37]] and [91Fla, [40]] are represented.

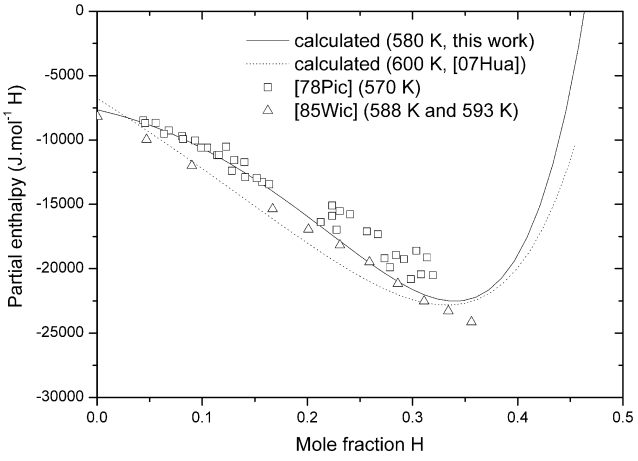

Fig. 3. Partial enthalpy at high temperature as a function of composition in the Pd–H system. Experimental data from [78Pic, [38]] and [85Wic, [39]] are represented.

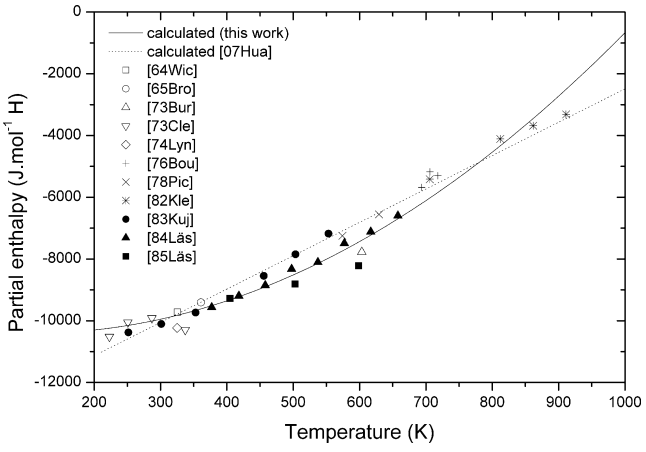

Fig. 4. Partial enthalpy at infinite H dilution as a function of temperature in the Pd–H system. The experimental data are redrawn from [20].

miscibility gap. The estimated critical point is located at $x_c = 0.190$, $T_C = 566$ K, in good agreement with experimental data (see 2.1.1). The calculated spinodal curve is shown. The calculated partial enthalpies as a function of composition at 298 K and 580 K (this later temperature being above the miscibility gap) is shown in Figs. 2 and 3 and compared with the experimental data [37–40].

It is shown also at infinite dilution and as a function of temperature in Fig. 4 compared to experimental data. Most of the plotted data have not been taken into account during the optimization since they are values derived from the pressure–composition curves. One may appraise the non-constant and non-linear behaviour justifying the use of the terms in $T\ln(T)$ and T^2 in the description of $G^{fcc}_{Pd:H}$.

Selected pressure–composition curves in the hydrogen-poor region and in the complete composition range are shown in Figs. 5 and 6 again in comparison with experimental data. One may notice the very good agreement with the plotted experimental data in the hydrogen-poor region. Note that the agreement is also very good with the other data (not plotted) for example from Refs. [23,30,33].

As already discussed the true equilibrium plateau pressure lies between absorption and desorption curves. This equilibrium calculated value of the plateau pressure is plotted in Fig. 7 as a function of temperature.

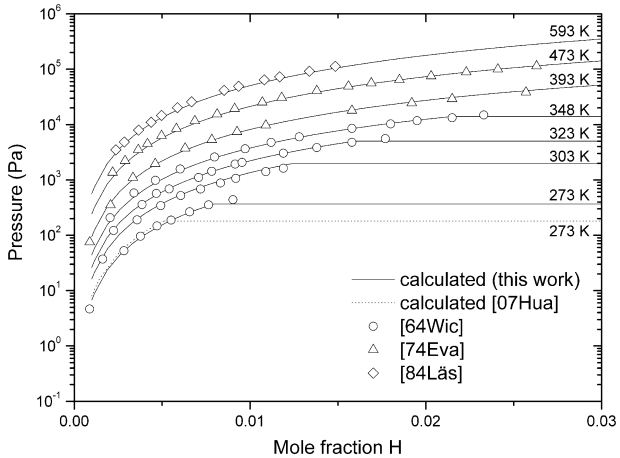

Fig. 5. Pressure–composition curves at low H concentration in the Pd–H system. Selected experimental data from [64Wic, [22]], [74Eva, [31]] and [84Läs, [32]] are represented.

As one may see from the different figures, the agreement is quite good with most experimental data. A comparison of our assessment can be made with the assessment recently published

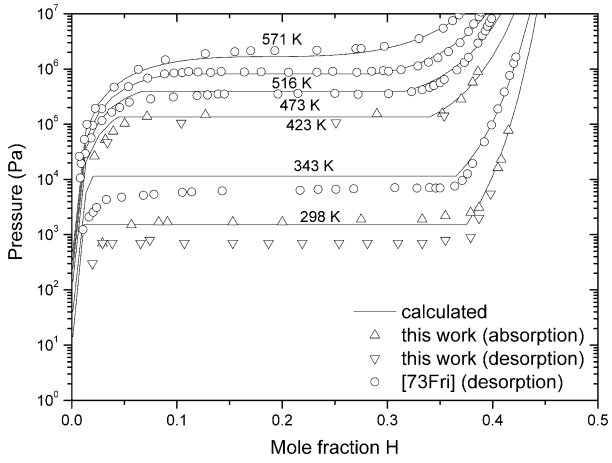

Fig. 6. Pressure–composition curves in the complete concentration range in the Pd–H system. Selected experimental data of [73Fri, [24]] and from this work are represented.

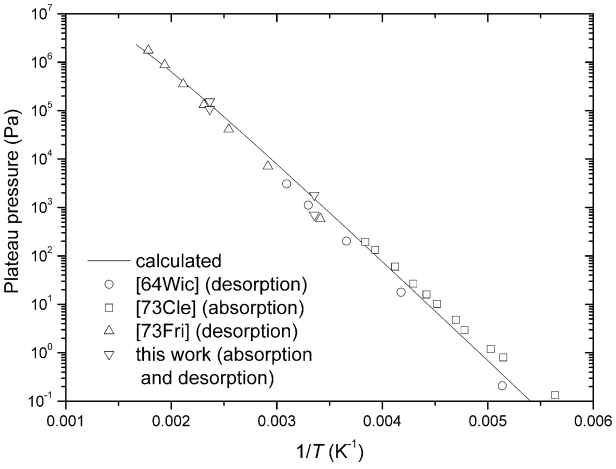

Fig. 7. Plateau pressure as a function of the inverse temperature in the Pd–H system. Experimental data of [64Wic, [22]], [73Cle, [30]], [73Fri, [24]] are represented.

by Huang et al. [9]. As can be inferred from Fig. 1, a better agreement of the phase diagram data has been obtained. In particular, the critical point assessed by these authors is clearly different from the one determined experimentally. The differences between the two assessments can be attributed to the smaller (and probably insufficient) number of parameters used by these authors (7 compared to 10 in our description) and to the choice to fit the desorption curves as the equilibrium curves instead of the calorimetric data (see Fig. 2) which are more representative of the real equilibrium because they do not depend on the direction of the reaction [40].

4.2. Pd–D system

The calculated phase diagram is shown in Fig. 8 and is compared to the experimental data. Several authors pointed out differences in the miscibility gap positions when measured in absorption or desorption [25,42]. The calculated line is found to be closer to absorption than desorption data. The critical point (x_c = 0.194, T_c = 566 K) is found to be very similar to the one determined for Pd–H system. The spinodal curve is also shown. Fig. 9 presents the most significant calorimetric data with the calculated ones. The data of Wicke at high deuterium concentration [39] have

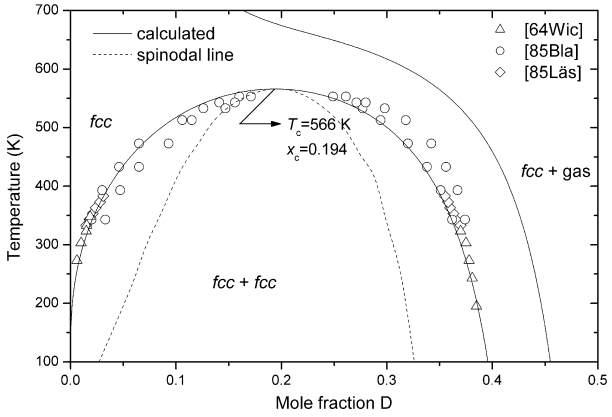

Fig. 8. Pd–D phase diagram at 1×10^7 Pa. The calculated spinodal line is shown. Experimental data from [64Wic, [22]], [85Bla, [42]] (absorption and desorption) and [85Läs, [41]] are represented.

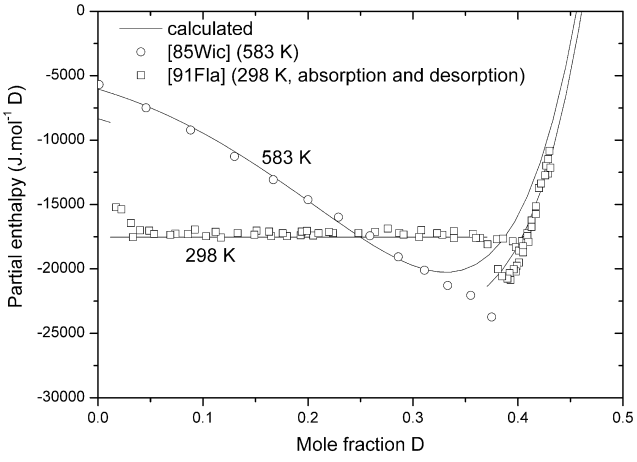

Fig. 9. Partial enthalpy at two temperatures as a function of composition in the Pd–D system. Experimental data from [85Wic, [39]] and [91Fla, [40]] (absorption and desorption) are represented.

been found to be incompatible with the data of Flanagan et al. and are impossible to reproduce (the partial enthalpy should reach a minimum and increase at higher deuterium concentration). The pressure–composition curves are plotted in Figs. 10 and 11 for low and high deuterium concentration with a selection of experimental data. The pressure plateau is shown in Fig. 12. Like for Pd–H system, a very good description of most experimental data is obtained by calculation.

4.3. Pd–T system

As much less data are available (in particular no calorimetric data), all the interaction parameters have been fixed to the values obtained for deuterium. Only the enthalpy and entropy of formation of the tritide PdT were optimized and were sufficient to describe well all the available data.

This choice is justified by the following reasons:

- these parameters do not differ very much from H to D and even smaller changes are expected between D and T because of the lower relative mass change between the isotopes;
- less data and especially no calorimetric data are available to stabilize the fit of so many parameters;
- less confidence can be placed in the experimental data due to the problems raised by the isotopic purity (some data have been corrected for this phenomenon, other have not and

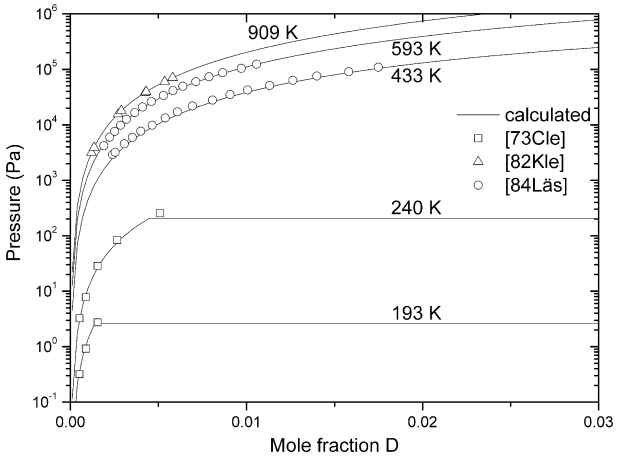

Fig. 10. Pressure–composition curves at low D concentration in the Pd–D system. Selected experimental data from [73Cle, [30]], [82Kle, [36]] and [84Läs, [32]] are represented.

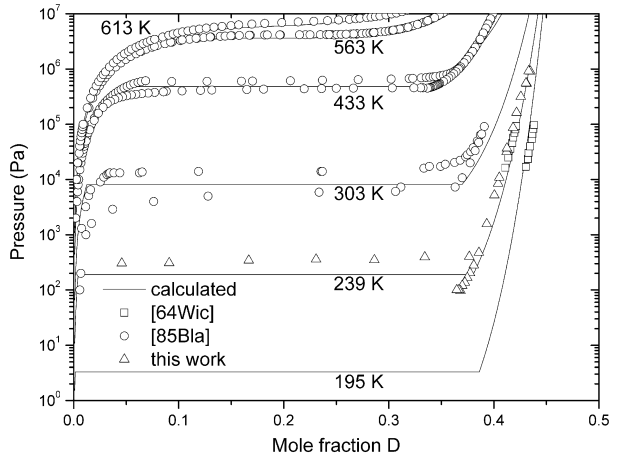

Fig. 11. Pressure–composition curves in the complete concentration range in the Pd–D system. Selected experimental data of [64Wic, [22]], [85Bla, [42]] (absorption and desorption) and from this work (absorption and desorption) are represented.

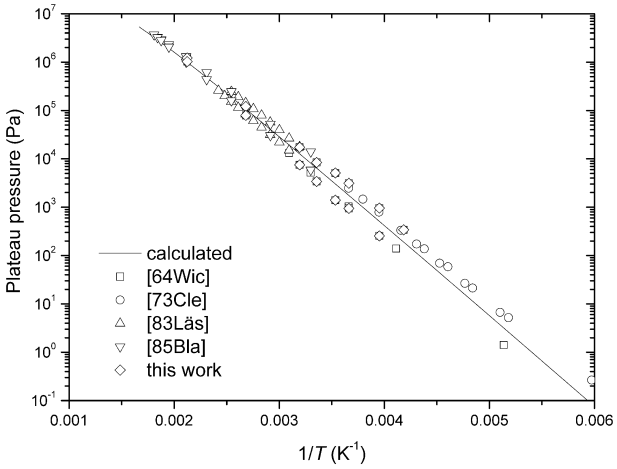

Fig. 12. Plateau pressure as a function of the inverse temperature in the Pd–D system. Experimental data of [64Wic, [22]], [73Cle, [30]], [83Läs, [44]], [85Bla, [42]] and this work are represented.

for some data the isotopic purity is not specified), by ^{3}He pollution and by the specific experimental procedures that should be used to handle this isotope;
- a good fit to most data was obtained with this set of parameters and did not justify to change anything (a refinement of some parameters did not improve much the description, on the contrary, a tendency to divergence was observed when too much parameters were refined simultaneously).

In the course of the assessment, we found that the data of Schmidt and Sicking [45] were incompatible with those of Ref. [46]. They were finally discarded.

The phase diagram is shown in Fig. 13 again with the spinodal curve. The critical point is unchanged compared to Pd–D system. Selected pressure–compositions curves are shown in Figs. 14 and 15 in the tritium poor and rich regions. The plateau pressure is plotted in Fig. 16 as a function of temperature.

4.4. Comparison between the three binary systems

The calculated miscibility gaps in the three systems Pd–H, Pd–D and Pd–T are quite similar. In contrast with other works that found the critical point of the Pd–D system lower than the one of the Pd–H system [20], we find a very close value of the critical temperature. The previously assessed difference is probably much smaller than the uncertainty generated by the different limits of the miscibility gap observed in absorption and desorption. Too few data exist on the miscibility gap of Pd–T system to evaluate the critical temperature. As we have chosen to describe this system with the same interaction parameters as for the Pd–D system, the same miscibility gap and critical point are calculated. In contrast, the H, D or T solubility lines at a given pressure (compare Figs. 1, 8 and 13) and the pressure–composition curves for the three systems at a given temperature are strongly different. At 300 K, the ratio between the D and H plateau pressures is 4.2 while the ratio between T and H plateau pressure is 8.1. A close look to the parameters shows that the main difference between the three systems is the enthalpic term corresponding to the formation of PdH, PdD or PdT while, on the contrary, the interaction with vacancies in the second sublattices are quite independent on the isotope.

4.5. Pd–H–D–T

An extrapolation of the binary systems into the different ternaries can be performed. For this, the mixed species HD, HT and

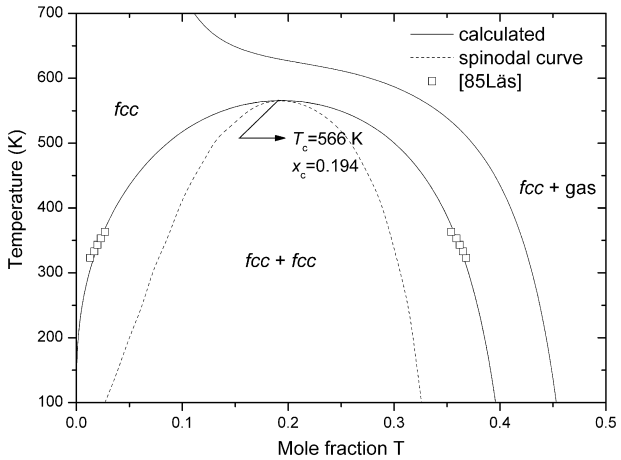

Fig. 13. Pd–T phase diagram at 1×10^7 Pa. The calculated spinodal line is shown. Experimental data from [85Läs, [41]] are represented.

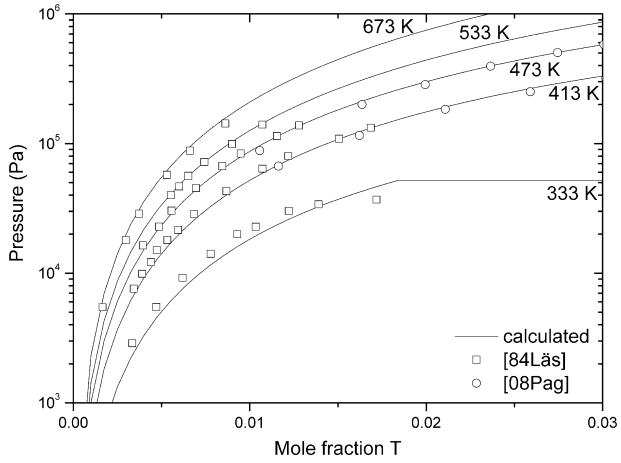

Fig. 14. Pressure–composition curves at low T concentration in the Pd–T system. Selected experimental data from [84Läs, [32]] and [08Pag, [50]] are represented.

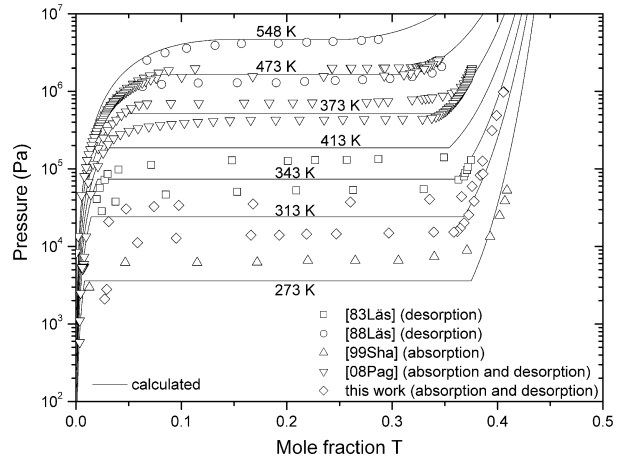

Fig. 15. Pressure–composition curves in the complete concentration range in the Pd–T system. Selected experimental data of [83Läs, [44]], [88Läs, [47]], [99Sha, [48]], [08Pag, [50]] and this work are represented.

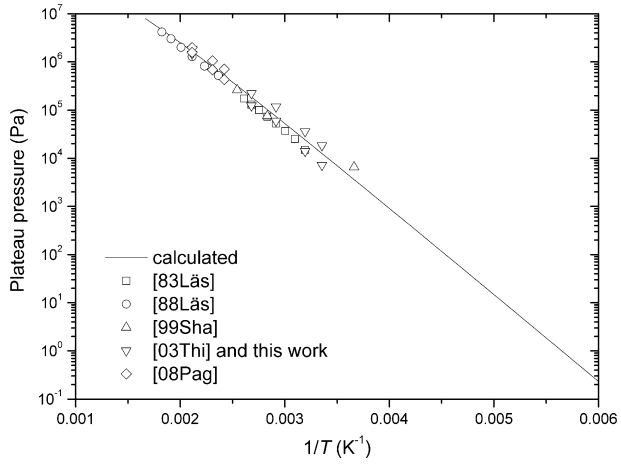

Fig. 16. Plateau pressure as a function of the inverse temperature in the Pd–T system. Experimental data of [83Läs, [44]], [88Läs, [47]], [99Sha, [48]], [03Thi, [49]], [08Pag, [50]] and this work are represented.

DT have to be considered in the gas phase. The ternary extrapolation of the Pd–H-D system at 300 K was first made in the frame of

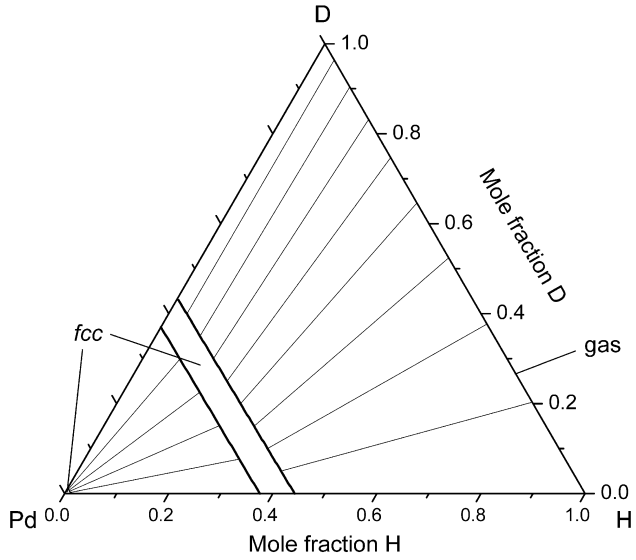

Fig. 17. Ternary isothermal section of the Pd–H–D system at 300 K and 1×10^7 Pa. The gas phase has no extension in the ternary field. The central *fcc* domain extends continuously from binary Pd–H to binary Pd–D system. Selected tie-lines (shown as thinner lines) represent the compositions in equilibrium in the two two-phase domains of the phase diagram (*fcc* + *fcc* and *fcc* + gas).

the classical model of extrapolation of Muggianu et al. [65]. Contrary to the expectation, the system develops a miscibility gap between the hydrogen rich and deuterium rich compositions of the solid phase. This feature is very unlikely. Though very difficult to evidence experimentally, it would produce anomalies on the isotope separation factor due to the presence of a tie-triangle joining these two compositions and the gas phase that were never put in light. In order to suppress the miscibility gap, a large negative ternary interaction parameter has to be introduced associated with the hydrogen–deuterium mixing. The physical meaning of such a parameter is difficult to apprehend since, hydrogen and deuterium being isotopes, they have no reason to interact chemically. In addition, with this model, the isotope separation factors measured experimentally could never be reproduced well.

In a second step, we realized that the interactions on the second sublattice of the model used for the solid are extremely dissymmetric, since this sublattice mixes two similar elements (H and D) with vacancies. As we have shown, the interaction between H and vacancies, on the one hand and D and vacancies on the other hand are strongly repulsive, while no interaction between H and D is expected. This is a typical example of a system which should be extrapolated following the Toop method [66], choosing vacancy as the Toop element. Additional analysis of the different extrapolation methods in ternary systems can be found in Refs. [67–69]. Such an extrapolation has been performed and gives a much more reasonable calculated isothermal section without the use of any ternary parameter (Fig. 17). A detailed analysis of the projection method used of Muggianu et al. [65] shows that the miscibility gap present in the former calculation is the projection of the miscibility gaps of the two binary systems Pd–H and Pd–D, since at a composition close to $PdH_{0.4}D_{0.4}$ very repulsive interaction parameters are extrapolated which is not the case with the Toop model.

Hydrogen preference for the solid phase compared to the gas phase can be appraised from the inclination of the tie-lines in Fig. 17 joining these two phases compared to lines passing by pure Pd which represent an equal distribution of H and D in the two phases. The corresponding isotope separation factor can be calculated numerically at any composition, pressure and temperature. It is shown in Fig. 18 as a function of composition and in Fig. 19

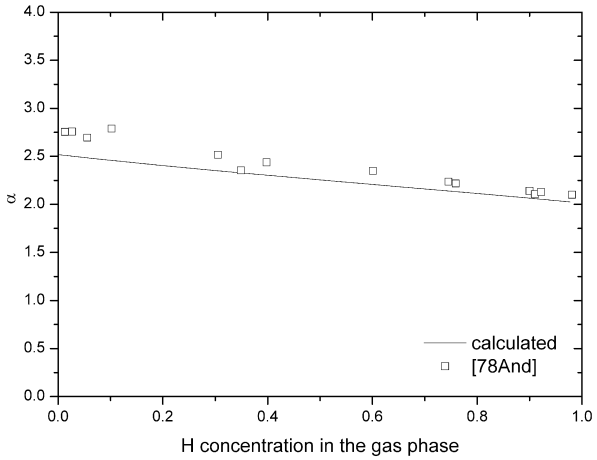

Fig. 18. Isotope separation factor in the ternary Pd–H–D system as a function of hydrogen concentration in the gas phase at $T = 273$ K and $P = 10^5$ Pa. Experimental data of [78And, [52]] are represented.

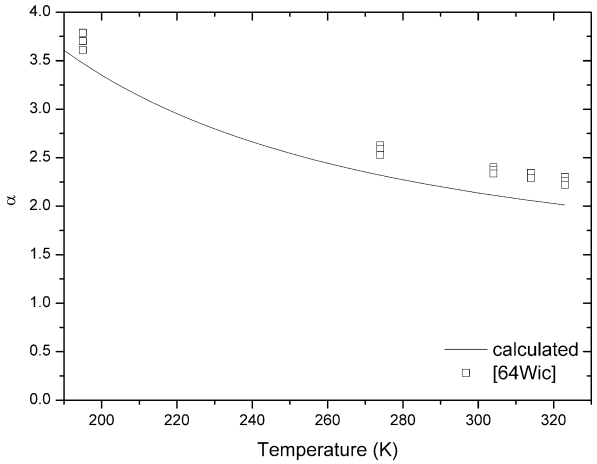

Fig. 19. Isotope separation factor in the ternary Pd–H–D system as a function of temperature at $P = 10^5$ Pa, $x_{Pd} = 0.5$, $x_H = 0.25$ and $x_D = 0.25$. Experimental data of [64Wic, [22]] are represented.

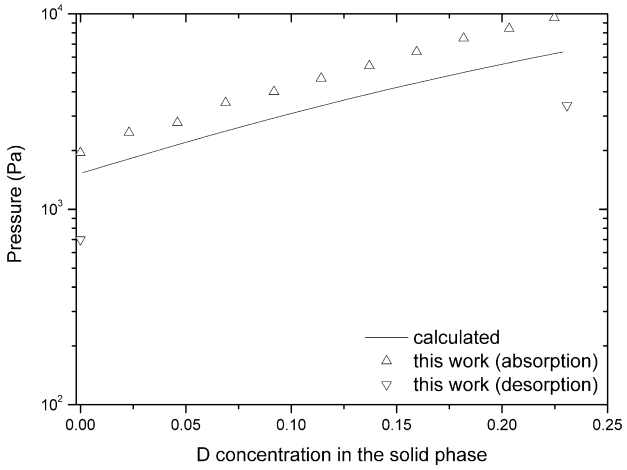

Fig. 20. Absorption pressure in the ternary Pd–H–D system at $x_H^{fcc} + x_D^{fcc} = 0.23$ as a function of x_D^{fcc} at 298 K.

as a function of temperature in comparison with experimental data. The agreement is quite good. We should note that the experimental details provided in the publication dealing with the separation factors are generally not sufficient to describe completely the equilibrium (lack of the overall quantity of the gas phase as compared to the solid phase), so that we are not sure that the calculation is strictly comparable to the experimental data.

Finally, we can compare the calculated plateau pressures for hydrogen–deuterium mixing and compare to the experimental values obtained in the present work (Fig. 20). Again the agreement is good, given the fact that only absorption data are reported for the ternary compositions while the calculation is done at the equilibrium *i.e.* between absorption and desorption.

The Pd–D–T and Pd–H–T systems ternary diagrams can be calculated in a similar manner (not shown). Any extrapolation can also be performed in the quaternary system Pd–H–D–T with good confidence.

5. Conclusions

As far as we are aware, this work is the first Calphad assessment of a system with different isotopes. As described in the introduction, metal hydrides are very suited for this kind of work, since the isotope effect is indeed very large. Not only a good description of the three binary systems Pd–H, Pd–D and Pd–T have been obtained, but also good estimations could be obtained by projection in the higher order systems without the use of any ternary interaction parameter, as expected from the chemical identity of the three isotopes. This kind of calculation allows in particular the determination of the isotope separation coefficient which can be of very high interest. It has been discovered major differences between extrapolations made with the conventional Muggianu model [65] and with the Toop model [66]. This effect is often disregarded and should perhaps be looked into more details in other systems. To our knowledge, this is the first time that the Toop model is used for the modelling of a solid phase described within the sublattice model.

References

[1] N. Dupin, I. Ansara, C. Servant, C. Toffolon, C. Lemaignan, J.-C. Brachet, J. Nucl. Mater. 275 (1999) 287–295.
[2] K. Zeng, T. Klassen, W. Oelerich, R. Bormann, Int. J. Hydrogen Energy 24 (1999) 989–1004.
[3] Kejun Zeng, T. Klassen, W. Oelerich, R. Bormann, J. Alloys Compd. 283 (1999) 213–224.
[4] Kejun Zeng, T. Klassen, W. Oelerich, R. Bormann, J. Alloys Compd. 283 (1999) 151–161.
[5] E. Königsberger, G. Eriksson, W.A. Oates, J. Alloys Compd. 299 (2000) 148–152.
[6] C. Qiu, G. Olson, S.M. Opalka, D.L. Anton, J. Phase Equilibr. Diffus. 25 (6) (2004) 520–527.
[7] J.-W. Jang, J.-H. Shim, Y.W. Cho, B.-J. Lee, J. Alloys Compd. 420 (2006) 286–290.
[8] B.-M. Lee, J.-W. Jang, J.-H. Shim, Y.W. Cho, B.-J. Lee, J. Alloys Compd. 424 (2006) 370–375.
[9] W. Huang, S.M. Opalka, D. Wang, T.B. Flanagan, Calphad 31 (3) (2007) 315–329.
[10] M. Palumbo, F.J. Torres, J.R. Ares, C. Pisani, J.F. Fernandez, M. Baricco, Calphad 31 (2007) 457–467.
[11] Shusuke Ukita, Hiroshi Ohtani, Mitsuhiro Hasebe, J. Jpn. Inst. Met. 71 (9) (2007) 721–729.
[12] S. Ukita, H. Ohtani, M. Hasebe, Adv. Mater. Res. 26–28 (2007) 989–992.
[13] C. Qiu, S.M. Opalka, O.M. Løvvik, G.B. Olson, Calphad 32 (2008) 624–636.
[14] S. Ukita, H. Ohtani, M. Hasebe, Mater. Trans. 49 (11) (2008) 2528–2533.
[15] M. Palumbo, J. Urgnani, D. Baldisson, L. Battezzati, M. Barricco, Calphad 33 (1) (2009) 162–169.
[16] K.L. Shanahan, J.S. Holder, J. Alloys Compd. 446–447 (2007) 670–675.
[17] S. Thiébaut, M. Douilly, S. Contreras, B. Limacher, V. Paul-Boncour, B. Décamps, A. Percheron-Guégan, J. Alloys Compd. 446–447 (2007) 660–669.
[18] E. Wicke, H. Brodowsky, in: G. Allefeld, J. Vökl (Eds.), Topics in Applied Physics, Hydrogen in Metals II, vol. 29, Springer-Verlag, Berlin, Heidelberg, New York, 1978, pp. 73–155.
[19] T.B. Flanagan, W.A. Oates, Annu. Rev. Mater. Sci. 21 (1991) 269–304.

[20] F.D. Manchester, A. San-Martin, J.M. Pitre, J. Phase Equilibr. 15 (1) (1994) 62–83.
[21] Y. de Ribaupierre, F.D. Manchester, J. Phys. C: Solid State Phys. 7 (1974) 2126–2139.
[22] v.E. Wicke, G.H. Nernst, Ber. Bunsen-Ges. 68 (3) (1964) 224–235.
[23] J.W. Simmons, T.B. Flanagan, J. Phys. Chem. 69 (11) (1965) 3773–3781.
[24] H. Frieske, E. Wicke, Ber. Bunsen-Ges. 77 (1) (1973) 48–52.
[25] E. Wicke, J. Blaurock, J. Alloys Compd. (130) (1987) 351–363.
[26] J.E. Worsham Jr., M.K. Wilkinson, C.G. Shull, Phys. Chem. Solids 3 (1957) 303–310.
[27] G. Nelin, Phys. Status Solidi (b) 45 (1971) 527–536.
[28] M.P. Pitt, E.M. Gray, Europhys. Lett. 64 (3) (2003) 344–350.
[29] A. Sieverts, Z. Phys. Chem. (60) (1907) 129–201.
[30] J.D. Clewley, T. Curran, T.B. Flanagan, W.A. Oates, J. Chem. Soc. Faraday Trans. I 69 (1973) 449–458.
[31] M.J.B. Evans, Can. J. Chem. 52 (1974) 1200–1205.
[32] R. Lässer, Phys. Rev. B 29 (8) (1984) 4765–4768.
[33] S. Luo, T.B. Flanagan, J. Alloys Compd. 419 (2006) 110–117.
[34] N.N. Kalinyuk, Russ. J. Phys. Chem. 54 (11) (1980) 1611–1613.
[35] G. Boureau, O.J. Kleppa, J. Chem. Phys. 65 (10) (1976) 3915–3920.
[36] O.J. Kleppa, R.C. Phutela, J. Chem. Phys. 76 (2) (1982) 1106–1109.
[37] J.F. Lynch, T.B. Flanagan, J. Chem. Soc. Faraday Trans. I 70 (1974) 814–821.
[38] C. Picard, O.J. Kleppa, G. Boureau, J. Chem. Phys. 69 (12) (1978) 5549–5556.
[39] E. Wicke, Z. Phys. Chem. Neue Folge 143 (1985) 1–21.
[40] T.B. Flanagan, W. Luo, J.D. Clewley, J. Less-Common Met. 172–174 (1991) 42–55.
[41] R. Lässer, J. Phys. Chem. Solids 46 (1) (1985) 33–37.
[42] J.G. Blaurock, Thermodynamik und Zustandsdiagramm des Pd/D_2-Systems im Vergleich zu Pd–H_2 und magnetisches Verhalten dieser Systeme, Thesis, Wilhems-University, Munster, Germany CB10072a, 1985.
[43] G. Boureau, O.J. Kleppa, P. Dantzer, J. Chem. Phys. 64 (12) (1976) 5247–5254.
[44] R. Lässer, K.-H. Klatt, Phys. Rev. B 28 (2) (1983) 748–758.
[45] S. Schmidt, G. Sicking, Z. Nat. Forsch. 33a (1978) 1328–1332.
[46] R. Lässer, J. Phys. F: Met. Phys. 14 (1984) 1975–1981.
[47] R. Lässer, T. Schober, Mater. Sci. Forum 31 (1988) 39–76.
[48] K.L. Shanahan, J.S. Holder, J.R. Wermer, J. Alloys Compd. 293–295 (1999) 62–66.
[49] S. Thiébaut, J. Demoment, B. Limacher, V. Paul-Boncour, B. Décamps, A. Percheron-Guégan, M. Prem, G. Krexner, J. Alloys Compd. 356–357 (2003) 36–40.
[50] S.N. Paglieri, D.J. Safarik, R.B. Schwarz, D.G. Tuggle, H. Oona, R.L. Quintana, E.L. Baron, Poster at the International Symposium on Metal–Hydrogen Systems, Reykjavik, Iceland, June 24–28, 2008.
[51] G. Sicking, Z. Phys. Chem. Neue Folge 93 (1974) 53–64.
[52] B.M. Andreev, A.S. Polevoi, A.N. Perevezentsev, Sov. At. Energy 45 (1) (1978) 710–716.
[53] F. Botter, J. Less-Common Met. 49 (1976) 111–122.
[54] H. Brodowsky, D. Repenning, Z. Phys. Chem. Neue Folge 114 (1979) 141–153.
[55] W. Luo, D. Cogwill, R. Causey, K. Stewart, J. Phys. Chem. B 112 (2008) 8099–8105.
[56] A. Sieverts, Z. Phys. Chem. B 38 (1937) 46–60.
[57] H.L. Lukas, S.G. Fries, B. Sundman, Computational Thermodynamics, the Calphad Method, Cambridge University Press, Cambridge, New York, Melbourne, Madrid, Cape Town, Singapore, São Paulo, 2007.
[58] H. Hemmes, A. Driessen, R. Griessen, J. Phys. C: Solid State Phys. 19 (1986) 3571–3585.
[59] B. Sundman, P. Shi, SGTE Pure Element Database, version 4.4, Thermo-Calc Software, Stockholm, 2002.
[60] B. Sundman, P. Shi, SSUB4 SGTE substance database, version 4.1, Thermo-Calc Software, Stockholm, 2002.
[61] B. Sundman, J. Ågren, J. Phys. Chem. Solids 42 (1981) 297–301.
[62] O. Redlich, A.T. Kister, Ind. Eng. Chem. 40 (2) (1948) 345–348.
[63] B. Sundman, B. Jansson, J.O. Andersson, Calphad 9 (2) (1985) 153–190.
[64] J.-O. Andersson, T. Helander, L. Höglund, P. Shi, B. Sundman, Calphad 26 (2) (2002) 273–312.
[65] Y.-M. Muggianu, M. Gambino, J.-P. Bros, J. Chim. Phys. 72 (1) (1975) 83–88.
[66] G.W. Toop, Trans. Metall. Soc. AIME 233 (1965) 850–855.
[67] M. Hillert, Calphad 4 (1) (1980) 1–12.
[68] P. Chartrand, A.D. Pelton, J. Phase Equilibr. 21 (2) (2000) 141–147.
[69] A.D. Pelton, Calphad 25 (2) (2001) 319–328.